Global Journal of Engineering and Technology Advances
eISSN: 2582-5003
Cross Ref DOI: 10.30574/gjeta
Journal homepage: https://gjeta.com/

(REVIEW ARTICLE)

Check for updates

Transient modes of high-speed rotor whit electric drive

Venelin Stoyanov Jivkov *

Department of Mechanisms and Machines Theory, Faculty of Industrial Technology, Technical University, Sofia.

Global Journal of Engineering and Technology Advances, 2022, 13(03), 008–021

Publication history: Received on 20 August 2022; revised on 29 September 2022; accepted on 02 October 2022

Article DOI: https://doi.org/10.30574/gjeta.2022.13.3.0151

Abstract

The paper presents the results of the study of the transient modes of a high-speed rotor with formally six degree of freedom, driven by an electric motor-generator during transition trough the resonance.

Based on the Newton-Euler equation, the differential equations of motion are derived, and the frequency spectrum of the considered electro-mechanical system is determined.

The following cases are considered: - transition trough resonance with unlimited (ideal energy source) and limited excitation by the motor; unstable frequency zones; phase trajectories and the influence of the electro-magnetic constant of the motor on the stability. The analysis of the stationary and nonstationary processes was carried out using the asymptotic method of Bogoliybov-Mitropolski. The stability of vibrations are determined by numerical solution of the equations in variations of the equilibrium states.

These transitions are of great importance for the recently widespread so-called uninterruptible power sources (UP), as well as the kinetic energy recovery system (KERS) used as additional propulsion energy .

Keywords: Rotor systems; Transient modes; Limited and Unlimited Excitation; Stability of Vibration

Highlights

- Stationary and non stationary vibrations of a high speed rotor, suspended in a homogeneous
- Elasto-dissipative field, under unlimited and limited excitation by the electric drive.
- Stability of vibrations during transition through resonance ; unstable frequency zones .
- Additional un-stability due to the dynamic characteristic of the engine; phases diagrams.

1. Introduction

Research into the transient modes of elementary centrifugal vibrators dates back to the beginning of the last century. While conducting experiments whit such electro-mechanical devices, the German physicist A. Sommerfeld observed unstable vibrations in certain speed ranges with slow change in the frequency of the exciting force [1]. He predicted, without the necessary precise evidence, that these phenomena were due to the interaction between the characteristics of electro motor and vibrating system.

Subsequently, this instability of vibrations (jump phenomenon) in the scientific literature received its citizenship as the Sommerfeld's effect. A few decades later [2],[3],[4],[5] gave a satisfactory physical explanation for this phenomenon, viz. the condition under which it occurs are defined.

* Corresponding author: V.S Jivkov
Department of Mechanisms and Machines Theory, Faculty of Industrial Technology, Technical University, Sofia.

The concepts of "limited" and " unlimited " excitation are introduced, depending on the type of (inclination or slope) of the static characteristic of the electric motor and the reduced moment of the resistance forces in the area of resonance states of the electro-mechanical system.

With „ unlimited „excitation, the transition through resonance is very fast, thanks to the large slope of the motor's characteristic (high starting moment).The higher the speed of the transition , the smaller the amplitudes of the forced vibrations, which is why unstable frequency zones do not exist [7],[8]. The transition through resonance of a „ limited „excitation of the electro-mechanical system is a relatively slow process due to the small slope of the static characteristic of the electric motor. Therefore, the small high-order terms an the right –hand sides of the equation describing rotation have the opportunity to manifest and they increase the reduced moment of resistance [8], [10].[11].

For planar centrifugal vibrators with two degrees of freedom (rotation and translation) the existence of unstable frequency zones in the resonance region has been proven experimentally and theoretically, depending on the type of intersection of the motor's moments and reduced resistances [8],[12].

Shortly before the resonance ,is observed an additional unstable zone due to the dynamic characteristic of the motor (.electro-magnetic inertia) [12].

The aim of the present research is the analysis transient modes in the vicinity of the first resonance of electro-mechanical rotor system with large kinetic moment JΩ, operating in the range between the first and second resonance.

In the recent times, the so called kinetic energy accumulators have massively entered the engineering practice as uninterruptible source of electricity (UPS), designed to drive a group of high-tech metalworking machines in the event of a power failure. [16], [17],[18]. These devices are an elastically suspended rotor with a build-in electric motor-generator, operating under conditions of „ unlimited „ excitation.

The other type - „limited „ excitation is applied to hybrid electric vehicles with a kinetic energy recovery system (KERS) – elastically suspended super flywheel, as additional drive system [19],[20],[21].

2. Theoretically consideration

Figure 1. Shows the elastically suspended rotor, as well as the selected coordinate systems: inertia, - X_0, Y_0, Z_0 ; fixed to the rotor X_3, Y_3, Z_3 and those with the indices 1 and 2 - determining its relative rotations.

2.1. Notation and basic dependencies

Coordinates - $\mathbf{y_1}$,$\mathbf{y_2}$,$\mathbf{y_3}$ defining radius vector $\overrightarrow{\rho_s}$ [m] ,

α, β and γ [-] rotation of the axis, where β and γ are small quantities.

$\mathbf{c}_1$, $\mathbf{c}_2$, $\mathbf{c}_3$ [N/m] , d_1 and d_2 [Ns/m] are elasto-dissipative coefficients ;

a and **b** [m] - the distance from the centers of the upper and lower bearing units to the plane X_3 ,O_3 ,Y_3.

M - Mass of the rotor [kg]; **ε** - eccentricity [m] ;β_r – dissipation coefficient [Nms]

J_3 - mass moment of inertia of the rotor [kgm^2] – A_3, A_3, C_3 – main, D_3,E_3,F_3 -centrifugal in coordinate system X_3 ,Y_3 ,Z_3.

In the following calculations, the next values of the physical and geometrical parameters of the electro-mechanical system, presented in the Fig. 1 are , used: $c_1 = c_2 = 5.10^5$ [N/m] ; $c_3 = 2.10^5$ [N/m] ;$d_1 = 1.10^3$ [Ns/m] ;$d_2 = 500$ [Ns/m] ; $d_3 = 250$ [Ns/m]; $d_4 = 1.10^{-4}$[Nms^2]; ε = 5.10^{-5} [m] ; a = 38.10^{-3} [m] ; b = 142.10^{-3} [m] ; $C_3 = 1.6$ [kgm^2] ; $D_3 = E_3 = 1.10^{-4}$ [kgm^2] ; $F_3 = 0$ [kgm^2] ; K =(0.05 - 2.0) [Nms] ; β = 150 [Nms] ; T = (0.00 – 0.35) [s]. $\beta_r = 18$ [Nms].

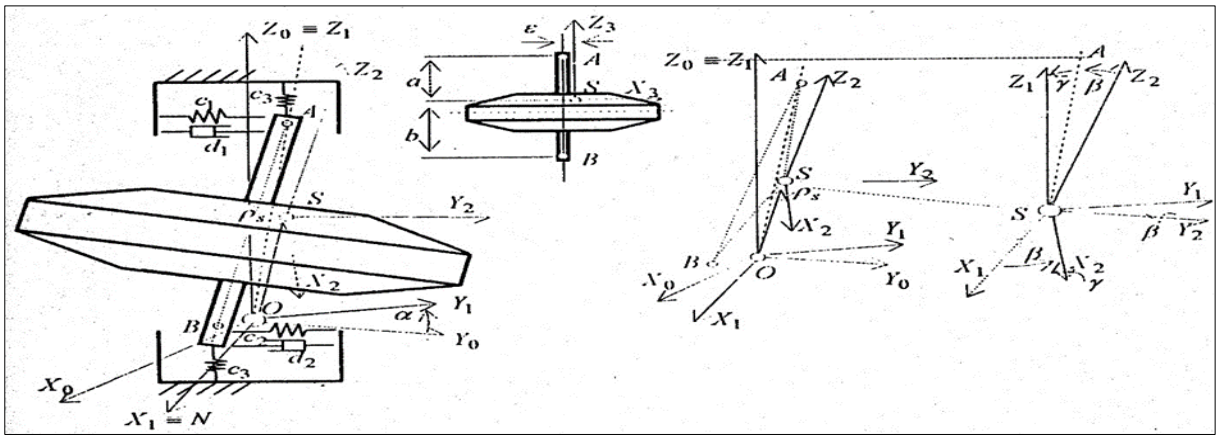

Figure 1 Elastically suspended rotor and its coordinate systems

Transfer matrix Δ_{ij} from the mobile X_3 , Y_3 and Z_3 coordinate system to the inertial one X_0 ,Y_0 ,Z_0 has the form [15]

$$\Delta_{ij} = \begin{vmatrix} \cos\alpha & -\sin\alpha & \chi \\ \sin\alpha & \cos\alpha & -\psi \\ -\beta & \gamma & 1 \end{vmatrix} \text{ where } \chi = \gamma\sin\alpha + \beta\cos\alpha; \psi = \gamma\cos\alpha - \beta\sin\alpha \tag{1}$$

The distances from the beginning O of the fixed coordinate system X_0 ,Y_0 ,Z_0 to the centers of the upper and lower bearing assembly, points A and B – Fig.1, are respectively equal to

$$O\vec{A} \equiv \vec{L}_A = \vec{\rho}_S + \Delta_{ij}.S\vec{A}; \vec{\rho}_S \equiv O\vec{S} = \begin{vmatrix} y_1 \\ y_2 \\ y_3 \end{vmatrix}; S\vec{A} = \begin{vmatrix} -\varepsilon \\ 0 \\ a \end{vmatrix}; O\vec{B} \equiv \vec{L}_B = \vec{\rho}_S + \Delta_{ij}.S\vec{B}; S\vec{B} = \begin{vmatrix} -\varepsilon \\ 0 \\ -b \end{vmatrix}. \tag{2}$$

After substituting (1) in (2) and regrouping, the next relations are obtained

$$O\vec{A} = \begin{vmatrix} O\bar{A}_x \\ O\bar{A}_y \\ OA_z \end{vmatrix} = \begin{vmatrix} y_1 - \varepsilon\cos\alpha + a\chi \\ y_2 - \varepsilon\sin\alpha - a\psi \\ y_3 + \chi a \end{vmatrix}; O\vec{B} = \begin{vmatrix} O\bar{B}_x \\ O\bar{B}_y \\ O\bar{B}_z \end{vmatrix} = \begin{vmatrix} y_1 - \varepsilon\sin\alpha - b\chi \\ y_2 - \varepsilon\sin\alpha + b\psi \\ y_3 - b\chi \end{vmatrix}. \tag{3}$$

Elasto-dissipative forces in bearing assembly can be represent with

$$\vec{F}_1 = \begin{vmatrix} -c_1.O\bar{A}_x - d_1.O\bar{A}_x^{\bullet} \\ -c_1.O\bar{A}_y - d_1.O\bar{A}_y^{\bullet} \\ -c_3.O\bar{A}_z \end{vmatrix}; \vec{F}_2 = \begin{vmatrix} -c_2.O\bar{B}_x - d_2.O\bar{B}_x^{\bullet} \\ -c_2.O\bar{B}_y - d_2.O\bar{B}_y^{\bullet} \\ -c_3.O\bar{B}_z \end{vmatrix}. \tag{4}$$

The moments of the forces with respect to mass center of the rotor can be written in the form

$$\vec{M}_1 = O\tilde{A}.\vec{F}_1; \vec{M}_2 = O\tilde{B}.\vec{F}_2; , \tag{5}$$

; where

$O\tilde{A}, O\tilde{B}$ are the co-symmetric tensors like this

$$O\tilde{A}=\begin{vmatrix} 0 & -O\bar{A}_y & O\bar{A}_z \\ O\bar{A}_y & 0 & -O\bar{A}_x \\ -O\bar{A}_z & O\bar{A}_x & 0 \end{vmatrix}; O\tilde{B}=\begin{vmatrix} 0 & -O\bar{B}_y & O\bar{B}_z \\ O\bar{B}_y & 0 & -O\bar{B}_x \\ -O\bar{B}_z & O\bar{B}_x & 0 \end{vmatrix}. \quad .(6)$$

The tensor of the mass moment of inertia of the rotor relative to the fixed coordinate system X_0 , Y_0 ,Z_0 in accordance with (1) is represented by

$$J_0 = \Delta_{ij}.J_3 \quad (7)$$

The absolute angular velocity $\vec{\omega}$ of the rotor in co-symmetrical form can be obtained from dependence [9]

$$\tilde{\omega}=\frac{d\,\Delta_{ij}}{dt}=\frac{d\Delta_{ij}}{dt}.\Delta_{ij}^{\ T}(T-transposed) \quad . \quad (8)$$

After processing and neglecting the small quantities of higher order, the final form of the angular velocity of the rotor with respect of the inertial coordinate system can be written as (9)

$$\omega=\left|\psi^{\bullet}+\chi.\alpha^{\bullet},\chi^{\bullet}-\psi.\alpha^{\bullet},\alpha^{\bullet}\right|^{T} \quad (9)$$

2.2. Equations of motion

After substituting the already obtained dependences for the mass moment of inertia J_0 - (7),for angular velocity $\vec{\omega}$ and $\tilde{\omega}$ - (8) and (9), for the acting forces and moments - $\vec{F}_1,\vec{F}_2,\vec{M}_1 and \vec{M}_2$ - (4) and (5) in the Newton-Euler [9] differential equations

$$J\vec{\omega}^{\bullet}+\tilde{\omega}.J.\vec{\omega}=\vec{M}_d-\vec{M}_r+\vec{M}_1+\vec{M}_2;\ \vec{M}_d=\begin{vmatrix} 0 \\ 0 \\ K(\Omega_0-\alpha^{\bullet}) \end{vmatrix}; \vec{M}_r=\begin{vmatrix} 0 \\ 0 \\ \beta_r.\alpha^{\bullet} \end{vmatrix}, \quad .(10)$$

$$\mathrm{M}.\ \vec{y}^{\bullet\bullet}=\vec{F}_1+\vec{F}_2,$$

The following system equations in scalar form, describing the motion of the elastically suspended rotor, is obtained like this

$$x_1^{\bullet\bullet}+a_1.x_1-a.x_2=-(h_1.x_1^{\bullet}+h_2.x_2^{\bullet})+N_1.e^{i(\alpha+\zeta)}$$

$$x_2^{\bullet\bullet}+(b_3-i.b_1).x_2-b_2.x_1=h_3.x_2^{\bullet}-h_4.x_1^{\bullet}+N_2.e^{i(\alpha+\eta)}$$

$$\mathrm{M}.\ y_3^{\bullet\bullet}+2.c_3.y_3=\varepsilon^2.f(a,b,c_1,c_2,d_1,...) \quad (11)$$

$$\alpha^{\bullet\bullet}=\frac{M}{C_0}-\frac{\beta}{C_0}.\alpha^{\bullet}-\frac{d_4}{C_0}.\alpha^{\bullet 2}+m_3.(\cos\alpha+\sin\alpha).\{(\chi^{\bullet\bullet}+\chi\alpha^{\bullet 2})-(\psi^{\bullet\bullet}+\psi\alpha^{\bullet 2})\};$$

$$TM^{\bullet}+M=K(\Omega_0-\alpha^{\bullet}),$$

$$x_1=y_1+i.y_2; x_2=\chi+i.\psi; i^2=-1,$$

where;
K – the slope of the engine's characteristic [Nms]]
Ω_0 – synchronous velocity [s^{-1}] .
T – electro-magnetic constant [s]

$$N_1 = \varepsilon.(a_1^{\,2} + h_1^{\,2}\alpha^{\bullet 2})^{1/2}; \zeta = arctg\,\frac{h_1\alpha^{\bullet}}{a_1}; N_2 = [(m_1\alpha^{\bullet 2} - \varepsilon b_2) + m_2\alpha^{\bullet 2}]^{1/2};$$

$$\eta = arctg\,\frac{m_2.\alpha^{\bullet 2}}{m_1.\alpha^{\bullet 2} - \varepsilon.b_2}; m_1 = \frac{E_0}{A_0}; m_2 = \frac{D_0}{A_0};\ \ m_3 = \frac{D_0}{C_0};$$

$$a_1 = \frac{c_1 + c_2}{\mathrm{M}}; a_2 = \frac{c_2.b - c_1}{\mathrm{M}}; b_1 = \frac{C_0}{A_0}; b_2 = \frac{c_2.b - c_1.a}{A_0}; b_3 = \frac{c_1.a^2 - c_2.b^2}{A_0}.$$

$$h_1 = \frac{d_1 + d_2}{\mathrm{M}}; h_2 = \frac{d_1 a - d_2 b}{\mathrm{M}}; h_3 = \frac{d_1 a^2 + d_2 b^2}{A_0}; h_4 = \frac{d_1 a - d_2 b}{A_0}.$$

3. Analytical solution

The free oscillations of the rotor can be obtained after zeroing the right parts of the first two equations of the system (11) and they have the form

$$x_j = A_k.\varphi_j^{(k)}.e^{i(\lambda_k t + \Phi_k)}; (j = 1,2), (k = 1,2). \qquad (12)$$

In essence the natural frequencies of the mechanical system of Fig.1 represent the real roots of the polynomial

$$\lambda^4 + b_1.\lambda^3 - (a_1 + b_3).\lambda^2 + a_1 b_1.\lambda + a_1 b_3 - a_2 b_2 = 0\ . \qquad (13)$$

This frequencies in our case are two real and two imaginary [14], [15] - see Fig.2 .

The modal vectors, or forms of the vibrations $\varphi^{(k)}{}_1$ and $\varphi^{(k)}{}_2$ can be obtained from next algebraic system equations

$$(-\lambda^2{}_k + a_1).\varphi^{(k)}{}_1 - a_2.\varphi^{(k)}{}_2 = 0 \qquad (14)$$

$$-b_2.\varphi^{(k)}{}_1 + (-\lambda^2{}_k + b_1.\lambda_k + b_3).\varphi^{(k)}{}_2 = 0\ ,$$

Where;

k – numbers of the corresponding frequency (k = 1,2)

The force nonstationary (transition) vibrations of the rotor in the vicinity of the first resonance k = 1, in accordance with the asymptotic method of Bogolyubov- Mitropolski [5] , [6], [10], [13] are sought in the form

$$x_j = A, \varphi_j^{(1)}.e^{i(\alpha + \Phi)}, \qquad (15)$$

where

$$\frac{dA}{dt} = \mu.A_1(\tau, A, \Phi); \frac{d\Phi}{dt} = \lambda + \mu.B_1(\tau, A, \Phi); and A, \Phi\ ... \qquad (16)$$

Are slowly changing function of time.

3.1. **Unlimited excitation („ ideal“energy source)** T=0.0, Ω_0 = 600,K = 0.25, d_4 = 0.0 – vacuum case; in the fourth equation of the system (11), small quantities of the second order are neglected.

You note by this conditions, that the last three equations in (11) are very weekly coupled to the coordinates x_1 and x_2 , and their solutions for an „ ideal „ energy source are practically trivial. Due this circumstances, the motion of the rotor is a very accurately described by the first two equations.

In compliance with the algorithm in this method [6], the function $A_1(\tau, A, \Phi)$ and $B_1(\tau, A, \Phi)$ are determined by the dependence

$$\{u_1(\lambda - \alpha^{\bullet})\frac{\partial A_1}{\partial \Phi} - (2\lambda_1 u_1 + u_2).B.A_1\} + i.\{u_1(\lambda_1 - \alpha^{\bullet}).A + \frac{\partial B_1}{\partial \Phi} +$$

$$+(2\lambda_1 u_1 + u_2).A_1 + A\frac{d(\lambda_1 u_1 - A.u_3}{d\tau}\} =$$

$$= \frac{1}{4\pi^2}\int_0^{2\pi}\int_0^{2\pi} N_1.e^{i(\alpha+\zeta)}.\varphi_1^{(1)}.e^{-i(\alpha+\Phi)}.d\alpha.d(\alpha+\Phi) + \quad (17)$$

$$+\frac{1}{4\pi^2}\int_0^{2\pi}\int_0^{2\pi} N_2.e^{i(\alpha+\eta)}.\varphi_2^{(1)}.e^{-i(\alpha+\Phi)}.d\alpha.d(\alpha+\Phi) -$$

$$-\frac{1}{4\pi^2}\int_0^{2\pi}\int_0^{2\pi} (h_1 x^{\bullet}_1 + h_2 x^{\bullet}).\varphi_1^{(1)}.e^{-i(\alpha+\Phi)} -$$

$$-\frac{1}{4\pi^2}\int_0^{2\pi}\int_0^{2\pi} (h_3 x^{\bullet}_2 - h_4 x^{\bullet}_1).\varphi_2^{(1)}.e^{-i(\alpha+\Phi)}.d\alpha.d(\alpha+\Phi),,$$

where;

$$u_1 = \varphi_1^{(1)^2} + \varphi_2^{(1)^2}; u_2 = b_2.\varphi_2^{(1)^2}; u_3 = b_2.\varphi_2^{(1)}.\frac{d\varphi_2^{(1)}}{d\tau}.$$

From the solutions of the double integrals $A_1(\tau, A, \Phi)$ and $B_1(\tau, A, \Phi)$ are determined by, which after substitution in (16) are finally represented by

$$A_1 = \{u_3 - \frac{d}{dt}(u_1.\lambda_1) - \frac{A\lambda_1[h_1.\varphi_1^{(1)^2} + (h_2+h_4).\varphi_1^{(1)}.\varphi_2^{(1)} + h_3.\varphi_2^{(1)^2}]}{2u_1\lambda_1 + u_2} -$$

$$-\frac{N_1.\varphi_1^{(1)}.\sin(\Phi-\zeta)}{u_1(\lambda_1+\alpha^{\bullet})+u_2} - \frac{N_2.\varphi_2^{(1)}.\sin(\Phi-\eta)}{u_1.(\lambda_1+\alpha^{\bullet})+u_2}\} \quad (18)$$

$$B_1 = -\frac{1}{A}\{\frac{N_1.\varphi_1^{(1)}.\cos(\Phi-\zeta)}{u_1(\lambda_1+\alpha^{\bullet})+u_2} + \frac{N_2.\varphi_2^{(1)}.\cos(\Phi-\eta)}{u_1(\lambda_1+\alpha^{\bullet})+u_2}\} .$$

After substitution (18) in (16), finally for $\frac{dA}{dt}$ and $\frac{d\Phi}{dt}$ can be written

$$\frac{dA}{dt} = -A.\frac{\delta_e}{2u_1\lambda_1 + u_2} - \frac{R\sin(\Phi - r)}{u_1(\lambda_1 + \alpha^{\bullet}) + u_2}; \frac{d\Phi}{dt} = \lambda_1 - \alpha^{\bullet} + \frac{R}{A}.\frac{\cos(\Phi - r)}{u_1(\lambda_1 + \alpha^{\bullet}) + u_2}, \quad (19)$$

where;

$$\delta_e = -u_3 + \frac{d(u_1.\lambda_1)}{dt} - \lambda_1.[h_1{\varphi_1}^{(1)^2} + (h_2 + h_4)\varphi_1\varphi_2 + h_3{\varphi_2}^{(1)^2}]$$

$$R = [(N_1.\varphi_1^{(1)}.\cos\zeta + N_2.\varphi_2^{(1)}.\cos\eta)^2 + (N_1.\varphi_1^{(1)}.\sin\zeta + N_2.\varphi_2^{(1)}.\sin\eta)$$

$$r = arctg[\frac{N_1.\varphi_1^{(1)}.\sin\zeta + N_2.\varphi_2^{(1)}.\sin\eta}{N_1.\varphi_1^{(1)}.\cos\zeta + N_2.\varphi_2^{(1)}\cos\eta}].$$

The stationary (steady - state) values of the amplitude-frequency characteristic of the mass center of the rotor in the vicinity (neighbour-hood) of the first resonance are obtained after zeroing the right parts of (19), or

$$\Phi_s = r + arctg\{\frac{-\delta_e}{(2u_1\lambda_1 + u_2).(\lambda_1 - \alpha^{\bullet})}. \quad (20)$$

$$A_s = \frac{R}{u_1(\lambda_1 + \alpha^{\bullet}) + u_2}.\frac{1}{[\frac{{\delta_e}^2}{(2u_1\lambda_1 + u_2)^2} + (\lambda_1 - \alpha^{\bullet}]^{\frac{1}{2}}}.$$

In the specific case, the real values of the natural frequencies in accordance with (13) are respectively $\lambda_1 = 340$ [s^{-1}] and $\lambda_2 = 1120$ [s^{-1}] ; [15] .

The next solutions are realized by forth order Runge-Kuta fixed step method and all initial conditions are set to zero

The calculated steady-state amplitude- frequency characteristic of the rotor's mass center, corresponding to the dependence (20) is shown in Fig.2 – with dashed line and denoted by – 1.

For the numerical solution of the differential system equations (19) , representing the transition through first resonance, it is preferable to introduce the following new variables

$$z_1 = A.\cos(\Phi - r); z_2 = A.\sin(\Phi - r) , \quad (21)$$

which actually eliminate the periodic function sin and cos.

In this case the system equations is transformed into

$$\frac{dz_1}{dt} = -\frac{\delta_e}{2u_1\lambda_1 + u_2} z_1 - (\lambda_1 - \alpha^{\bullet}).z_2 \quad (22)$$

$$\frac{dz_2}{dt} = -\frac{\delta_e}{2u_1 + u_2} z_2 + (\lambda_1 - \alpha^{\bullet}).z_1 + \frac{R}{A}.\frac{1}{u_1(\lambda_1 + \alpha^{\bullet}) + u_2} .$$

The transitions through the first resonance $\lambda_1 = \alpha^{\bullet}$ is proposed to be realized by linear change of the angular rotor's speed (23)

$$\alpha^{\bullet} = \alpha^{\bullet}_0 + \nu.t \quad , \tag{23}$$

where the speed gradients are two ν_1 and ν_2..

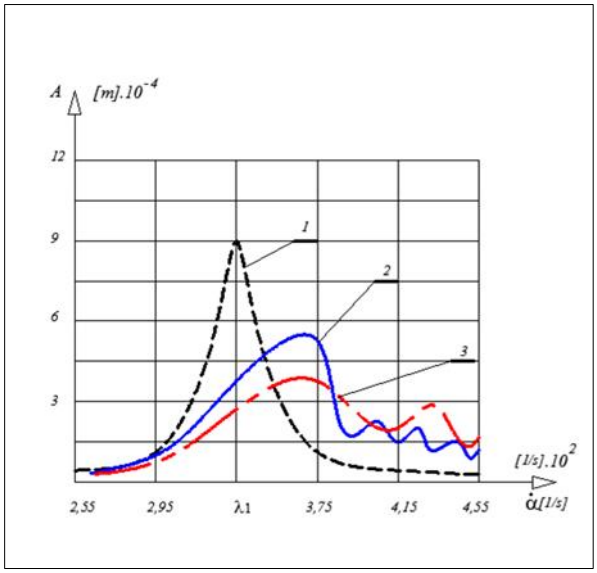

Figure 2 Amplitude-frequency characteristics of mass center S

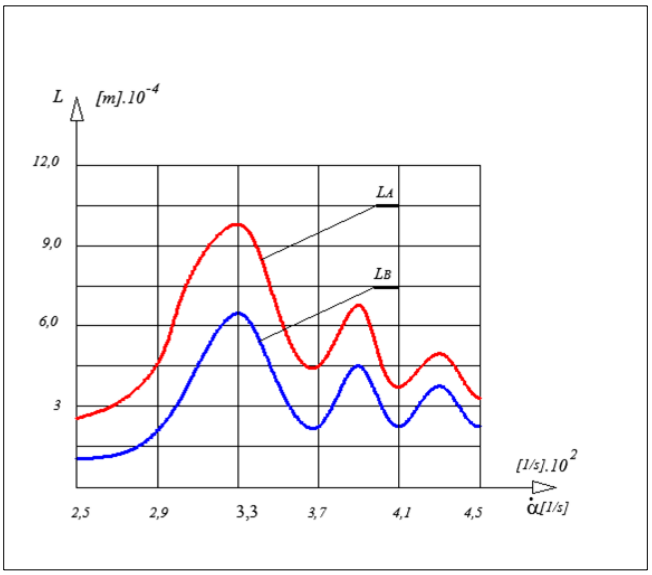

Figure 3 Amplitudes versus frequency of the upper LA and lower LB bearing units

Figure 2, at the same physical-geometrical parameters of the vibrating system, shows transition processes with ν_1= 500 [s^{-1}] – denoted by 2, and by ν_2=250 [s^{-1}] – denoted by - 3.

Amplitude –frequencies characteristics of the centers of the upper, respectively lower bearings units L_A and L_B can be express by relations

$$L_A = [A^2.(\varphi_1^{(1)} + a.\varphi_2^{(1)})^2 + \varepsilon^2 - 2A.(\varphi_1^{(1)} + a.\varphi_2^{(1)}).\varepsilon.\cos\Phi]^{\frac{1}{2}}.e^{i\alpha}.e^{i\frac{(\varphi_1^{(1)}+a.\varphi_2^{(1)})\sin\Phi}{(\varphi_1^{(1)}+a.\varphi_2^{(1)})\cos\Phi-\varepsilon}} \quad (24)$$

$$L_B = [A^2.(\varphi_1^{(1)} - b.\varphi_2^{(1)})^2 + \varepsilon^2 - 2.A.(\varphi_1^{(1)} - b.\varphi_2^{(1)}).\varepsilon.\cos\Phi]^{\frac{1}{2}}.e^{i\alpha}.e^{i\frac{(\varphi_1^{(1)}-b.\varphi_2^{(1)})\sin\Phi}{(\varphi_1^{(1)}-b.\varphi_2^{(1)})\cos\Phi-\varepsilon}},$$

and they are presented in Fig. 3 , at a velocity gradient ν = 500 [s^{-1}].

3.2. Limited excitation

This type of excitation of rotor systems with electric drive is typical for kinetic accumulators (KERS) used as an additional source of energy in modern electric automobiles, with very long time constant due to the „ soft „ characteristic (low slope) of the motor/generator.

In these electro-mechanical systems the small members of high order in the equation describing the rotation of the rotor – the fourth of (11), are manifested in the vicinity of the resonance and create conditions for un-stability of vibrations. For this particular case, the transition through resonance was considered in the following additional data

$$T = 0.2;\ K = 0.012;\ 800 < \Omega_0 < 1400..$$

Reapplying the algorithm of the asymptotic method [6], after α - averaging, the equations analogous to (19) are presented by

$$\frac{dA}{dt} = -\frac{A.\delta_e}{2\lambda_1 u_1 + u_2} + \frac{R}{u_1(\lambda_1 - \alpha^\bullet) + u_2}.\sin(\Phi - r);$$

$$\frac{d\Phi}{dt} = (\lambda_1 - \alpha^\bullet) - \frac{1}{A}.\frac{R}{u_1(\lambda_1 - \alpha^\bullet) + u_2}.\cos(\Phi - r); \quad (25)$$

$$\frac{d\alpha^\bullet}{dt} = \frac{M}{C_0} + A.[m_3\varphi_2(\alpha^{\bullet 2} - \lambda_1^{\ 2})(\cos\Phi - \sin\Phi) -$$

$$-\varepsilon(\alpha^\bullet + \lambda_1)(\varphi_1 h_7 + \varphi_2 h_8)\cos\Phi - \frac{h_6}{C_0}.\alpha^{\bullet 2};$$

$$\frac{dM}{dt} = -\frac{1}{T}[M + K(\alpha^\bullet - \Omega_0];\ .$$

Fig.4 presents the results for engine's moment – M, amplitude of the mass center S of the rotor - A and angular velocity - $\alpha^\bullet$ as a function of time, from numerical solution of the system differential equations (25). There is a significant reduction in engine's torque immediately after resonance. This is due to the transfer of energy from the gyroscopic moments of the rotor on the unbalanced by the elastic and dissipative forces α - coordinate. At the sometime the angular velocity of the rotor - $\alpha^\bullet$ increases due to the reduction of the main mass moment of inertia of the rotor of the preserved kinetic momentum.

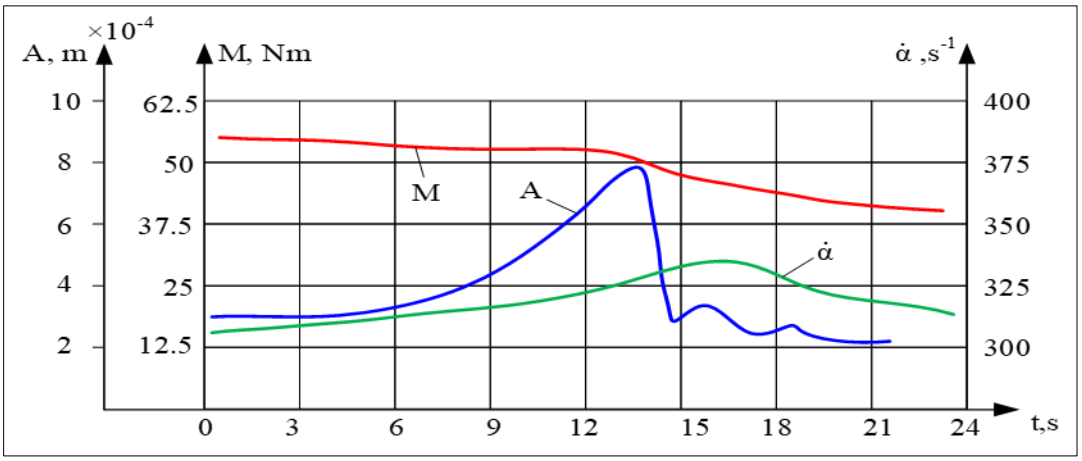

Figure 4 The transition through the first resonance

The steady- state(stationary) values of the parameters of vibrations at this type of excitation A_s , Φ_s , $\alpha^{\bullet}_s$ and M_s are obtained by resetting the left sides of the system equations (25) to zero, from which it follows that

$$M = K(\Omega_0 - \alpha^{\bullet}); ------ M = M(\alpha^{\bullet}); \quad , \qquad (26)$$

and the reduced resistance moment L ($\alpha^{\bullet}$) from the last but one (before the last) equation can to be represented by

$$L(\alpha^{\bullet}) = A[\varphi_2(\alpha^{\bullet 2} - \lambda_1^{\,2})].(D_0 \cos\Phi - E_0 \sin\Phi) - d_4\alpha^{\bullet 2} - \\ -\varepsilon.C_0(\lambda_1 + \alpha^{\bullet}).(\varphi_1 h_7 + \varphi_2 h_8).\cos\Phi; \qquad (27)$$

Figure 5 shows the two functions $M(\alpha^{\bullet})$ and $L(\alpha^{\bullet})$ for this electro-mechanical system in the range of ($300 \le \alpha^{\bullet} \le 800$) [$s^{-1}$] of the angular velocity of the rotor.

The unstable zones of vibrations can be determined at a quasi steady –state increase of the angular velocity of the rotor – from point 2 to point 1 (left oriented hatch) , and decrease – from point 1' to point 2' (right oriented hatch) – Fig.5. This corresponds to the jump phenomenon of the Sommerfeld's effect.by the well known relation for the stability of motion. [5],[13]

$$\frac{d\{M(\alpha^{\bullet}) - L(\alpha^{\bullet})\}}{d\alpha^{\bullet}} \updownarrow_{\alpha^{\bullet}_s} < 0 \qquad . \qquad (28)$$

It has been shown based on the experiments and theoretically [12] that for monotonic increase of the driving frequency, a jump phenomenon occurs at the beginning of the resonance ($0.8 \le \alpha^{\bullet} / \lambda \le 1.0$). The jump phenomenon is shown in Fig.5 - (horizontal hatching) . This effect can be explained by the singular excitation of the motor – the last equation in system (25), because the motor dynamic characteristic is unknown in explicit form [15].

The stability of vibrations and the form of the phase diagrams of the particular points can be determined exactly by analyzing the system equations (25) in variations.

The values of parameters of vibrations during the disturbed motion can be expressed in the form

$$A_1 = A + \Delta_1; \Phi_1 = \Phi + \Delta_2 : \alpha^{\bullet}_1 = \alpha^{\bullet} + \Delta_3; M_1 = M + \Delta_4 : \quad , \qquad (29)$$

where Δ_I (I = 1,2.3,4) are small deviations from the steady state values.

The variations form of (25) can be obtain by expanding these expressions in the Taylor series in the small parameters Δ_I , keeping only the linear terms

$$\frac{d\Delta_i}{dt} = \sum_1^4 b_{ij}.\Delta_j ; \Delta_i = \sum_1^4 \delta_i^{(k)}.C_i.e^{\lambda_k t}; \ , \tag{30}$$

where; b_{ij} are the coefficients in front of the linear terms in the expansions

$$b_{11} = \frac{1}{C_0\alpha^\bullet}\{\frac{dM}{d\alpha^\bullet} - 2b_6\alpha^\bullet + 2A\alpha^\bullet\varphi_2(D\cos\Phi - E\sin\Phi) +$$
$$+\varepsilon A[(d_1+d_2)\varphi_1 + (d_1a+d_2b)\varphi_2]\cos\Phi\} \quad ;$$

$$b_{12} = \frac{1}{C_0\alpha^\bullet}\{\varphi_2(\alpha^{\bullet 2} - \lambda_1^{\ 2})(D\cos\Phi - E\sin\Phi) +$$
$$+\varepsilon(\alpha^\bullet + \lambda_1)[(d_1+d_{\ 2})\varphi_1 + (d_1a+d_2b)\varphi_2]\cos\Phi\};$$

$$b_{13} = \frac{1}{C_0\alpha^\bullet}\{-A\varphi_2(\alpha^{\bullet 2} - \lambda_1^{\ 2})(D\cos\Phi - E\sin\Phi) -$$
$$-E\varepsilon(\alpha^\bullet + \lambda_1)[(d_1+d_2)\varphi_1 + (d_1a+d_2b)\varphi_2]\sin\Phi\};$$

$$b_{14} = \frac{1}{C_0\alpha^\bullet}; b_{24} = 0; b_{34} = 0; b_{41} = -\frac{K}{\alpha^\bullet}; b_{43} = 0; b_{42} = 0; b_{44} = \frac{1}{T\alpha^\bullet};$$

$$b_{22} = -\frac{\delta_e}{\alpha^\bullet(2\lambda_1u_1 + u_2)}; b_{23} = \frac{A(\lambda_1 - \alpha^\bullet)}{\alpha^\bullet}; b_{31} = -\frac{1}{\alpha^\bullet};$$

$$b_{32} = -\frac{\delta_e}{\alpha^\bullet(2\lambda_1u_1 + u_2)}; b_{33} = \frac{(\lambda_1 - \alpha^\bullet)}{A_0\alpha^\bullet}; \ .$$

The forms of the phase diagrams of the particular points can be derived from the generalized solution of (30) in the form

$$\Delta_i = \sum_1^4 \gamma_i^{\ (j)}.C_j.e^{\lambda t}, \tag{31}$$

where λ is the natural frequency of the system, C_j are constants of integration depending on initial conditions, $\gamma_i^{\ j}$ are fundamental function of $\left\|b_{ij} - \lambda.E\right\|$.

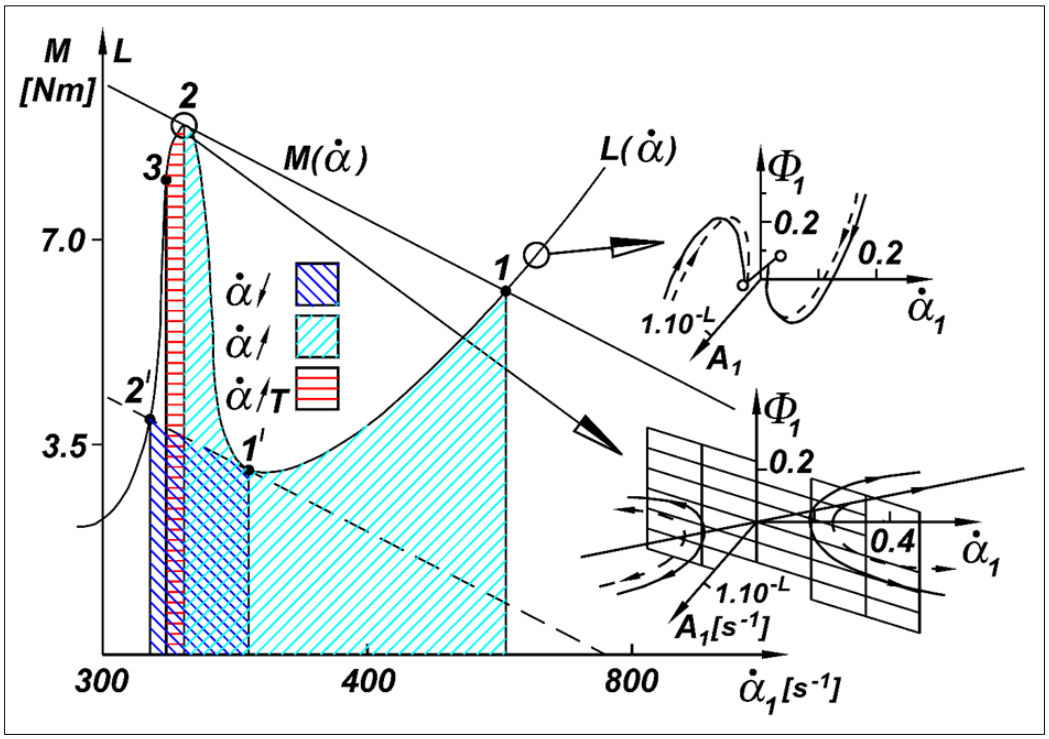

Figure 5 Unstable zones during quasi steady state transition through the first resonance

In the right upper part of the Fig 5 is shown phase diagram of the stable vibrations - stable focus, obtained from solution of (31).

For example the phase diagram for particular point 2 in Fig.5 is shown down right - saddle focus first order - unstable vibrations. The width of the add zone of instability of the vibration (points 2-3) on Fig.5 depends on the electro-magnetic motor's time- constant T [12].

Figure 6 shows the experimental record of the vibrations in the horizontal plane on the upper bearing assembly of the kinetic energy storage system. This diagram is given in the regime of a slow increase of the driving frequency. This result confirms the presence of the jump phenomenon in the rotor systems possessing large mass m moment of inertia.

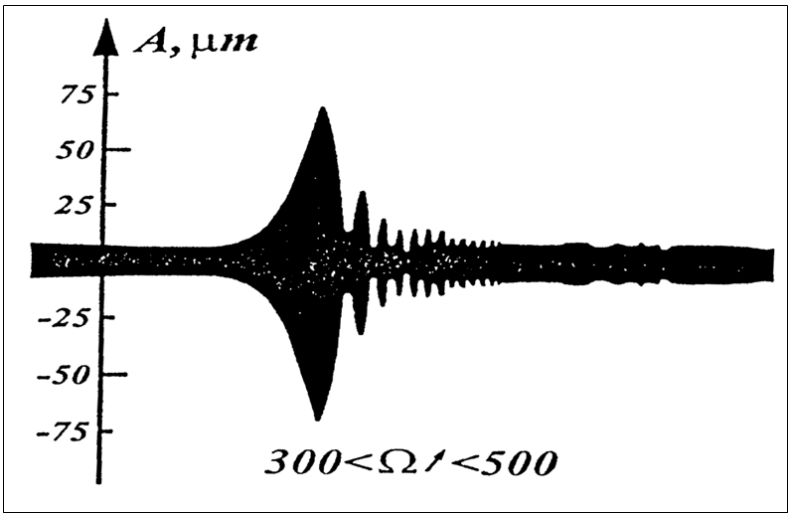

Figure 6 Experimental recording of the unstable vibrations after the resonance

4. Conclusion

The maximum amplitudes of the vibrations , the both at the rotor's mass center and at its bearing assemblies during the transition through resonance in the case of „ideal" energy source are significantly smaller and are shifted in direction of increasing the speed of rotation .

It is observed after passing the first maxima of attenuating (reducing in value) vibrations without the presence of unstable frequency zones.

The obtained results are prerequisite for optimization of forces F_1, F_2 -(4) and moments M_1 and M_2 - (5), both in steady state and transient modes of rotor's system.

Limited excitation „ in the neighbor-hood of the basic resonances have to be determined by analyzing and solving the system equations in variations during the disturbed motion.

Compliance with ethical standards

Acknowledgments

This work was supported by the European Regional Development Fund within the Operational Program "Science and Education for Smart Growth 2014 - 2020" under the Project CoE "National center of mechatronics and clean technologies "BG05M2OP001-1.001-0008- C0.

References

[1] Sommerfeld A., VDI № 18 pp. 631 – 636, 1904. (in German)

[2] Timoshenko S., Theory of Vibrations in Engineering GNTI M. 1931 (in Russian).

[3] Lewis F., Vibration during acceleration through critical speed – Bull. ASME. 1932 , 5 , № 23

[4] Katz N., Forced vibrations during resonance, Eng. Proceeding, vol.3 №2 Moskow 1947. (in Russian).

[5] Rocard Y., Dynamique generale des vibrations – Paris, Masson 1949, pp.437

[6] Bogolliubov N., Perturbation Theory in Nonlinear Mechanics , Collection of works of Building Mechanics Institute – 1950 № 4pp. 9-34, (in Russian).

[7] Mazet R., Mechanique vibratoire . Paris – Liege, Libr. Politechn Ch. Beranger 1955, pp. 358..

[8] Kononenko V., Resonance properties of the centrifugal vibrator. Proceedings of the Institute of Mechanical Science of Academy- M. 1958 № 71 pp.22 – 42, in Russian).

[9] Lurie A., Analytical Mechanics, Publishing House GimphL M. 1861 in Russian).

[10] Mitropolsky Y., Problems of the asymptotic theory of the nonstationary vibrations , Publishing House „ Science „ M. 1964 (in Russian)

[11] Tondl A., Dynamics of Rotors in Turbo-generators, Publishing House "Energy", Leningrad 1971.. (in Russian).

[12] Jivkov V. Influence of the electro-magnetic inertia of the engine on the stability of a mechanical system with centrifugal exciter., Proceedings of the Institute of Mechanical Science of Academy – M. № 4 ,pp. 12 – 18 , 1971. (in Russian).

[13] Shen S., F.Veldbaus Analysis and control of a flywheel hybrid vehicular powertrain, IEEE Trans – Control System Technology 2004, 12 645 660.l

[14] Abrahasson J. et al., On the efficiency of a two-Power-Level Flywheel – Based – All-Electric Driveline, Journal Energies ISSN № 19961073 №5,2012.

[15] Jivkov V. , Some singularity in Rotor's Systems with limited excitation, Comptes rendus de l'Academie Bulgare des Sciences, Tome 69 № 3, 2016.

[16] Jivkov V., et al., Combined Flywheel Suspension in stationary Kinetic Storage Systems (Patent), Official Bulletin of the Patent Agency № 01.1 from 17.01.2022. (in Bulgarian).

[17] www.kstar.com

[18] power@baykee.net

[19] www.powerthru.com

[20] www.kinetiktraction.com

[21] www.ricardo.com/en-GB/